

Supplementary Materials

Selective syngas conversion to olefins over bifunctional $\text{Zn}_2\text{Al}_3\text{O}_4/\text{PLS-3}$ catalyst

Jie Tuo¹, Xianchen Gong¹, Zhenteng Sheng¹, Qi Yang¹, Hao Xu^{1,2,*}, Yejun Guan^{1,2}, Peng Wu^{1,2,*}

¹State Key Laboratory of Petroleum Molecular & Process Engineering, Shanghai Key Laboratory of Green Chemistry and Chemical Processes, School of Chemistry and Molecular Engineering, East China Normal University, Shanghai 200062, China.

²Institute of Eco-Chongming, Shanghai, 202162, China.

***Correspondence to:** Prof. Hao Xu, Prof. Peng Wu, State Key Laboratory of Petroleum Molecular & Process Engineering, Shanghai Key Laboratory of Green Chemistry and Chemical Processes, School of Chemistry and Molecular Engineering, East China Normal University, No. 3663 North Zhongshan Road, Shanghai 200062, China. E-mail: hxu@chem.ecnu.edu.cn; pwu@chem.ecnu.edu.cn

EXPERIMENTAL

Chemicals and reagents

$\text{Al}(\text{NO}_3)_3 \cdot 9\text{H}_2\text{O}$ (AR, Shanghai Macklin Biochemical Co., Ltd.), NaOH (Sinopharm Chemical Reagent Co., Ltd.), $\text{Zn}(\text{NO}_3)_2 \cdot 6\text{H}_2\text{O}$ (AR, Shanghai Macklin Biochemical Co., Ltd.), sodium aluminate (AR, Aladdin), $(\text{NH}_4)_2\text{CO}_3$ (AR, Sinopharm Chemical Reagent Co., Ltd.), NH_4Cl (AR, Aladdin), tetraethyl ammonium hydroxide solution (TEAOH, 35 wt.%, Shanghai Macklin Biochemical Co., Ltd.), CH_2Cl_2 (GC, Sinopharm Chemical Reagent Co., Ltd.), HF (40 wt.% in water, Shanghai Macklin Biochemical Co., Ltd.), hexachloroethane (AR, Sinopharm Chemical Reagent Co., Ltd.), silica sol (30 wt.%, Aladdin), and piperidine (GC, Sinopharm Chemical Reagent Co., Ltd.) were all used as received without further purification.

Preparation of catalyst

FER zeolite with bulk crystal morphology was synthesized as a control sample via hydrothermal method. 0.31 g NaAlO_2 (53.12 wt.% Al_2O_3 , 41.52 wt.% Na_2O) and 0.39 g sodium hydroxide were added in 20 g deionized water. Then, 10.0 g silica sol, 0.85 g piperidine (PI) was added in the above solution, and obtained solution was stirred. The initial gel molar composition was 1.0 SiO_2 : 0.033 Al_2O_3 : 0.2 PI: 0.13 Na_2O : 30 H_2O . The gel was crystallized at 423 K for 7 d. Subsequently, the solid products were purified by filtration, washed with deionized water, dried at 353 K for 12 h and calcined at 823 K for 6 h. The FER zeolite was ion-exchanged in 1 M NH_4Cl solution (the mass ratio of solid/liquid = 1 : 50) and the process was repeated for 3 times under stirring at 353 K for 3 h. Finally, NH_4 -form FER was calcined at 823 K for 6 h to obtain H-FER zeolites.

The $\text{Zn}_2\text{Al}_3\text{O}_4$ oxide was used to couple with PLS-3 zeolite, forming the bifunctional catalysts for syngas conversion. $\text{Zn}_2\text{Al}_3\text{O}_4$ was synthesized by coprecipitation method following the previously reported method.¹ In brief, solution A was prepared by dissolving 23.5 g $(\text{NH}_4)_2\text{CO}_3$ in 150 g H_2O and solution B was prepared by dissolving 37.5 g $\text{Al}(\text{NO}_3)_3 \cdot 9\text{H}_2\text{O}$ and 29.75 g $\text{Zn}(\text{NO}_3)_2 \cdot 6\text{H}_2\text{O}$ in 150 g H_2O . Solution A and solution B were simultaneously added dropwise into a breaker under vigorous stirring at 343 K while keeping the pH value of mixture around 7 by adjusting the relative addition rates of the two solutions. After aging for 3 h at 343 K, the solid product was filtrated, dried at 373 K for 12 h and further calcined at 773 K for 4 h.

Characterization methods

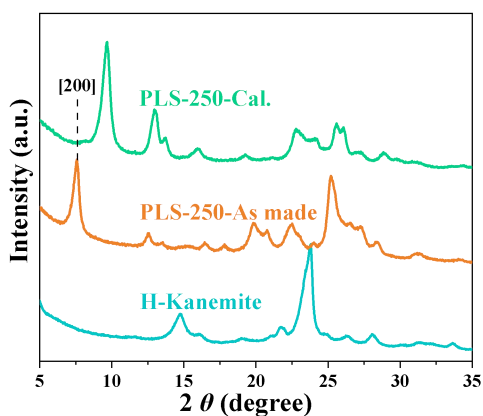
A Rigaku Ultima IV X-ray diffractometer with Cu-K α radiation ($\lambda = 1.5405 \text{ \AA}$) was used to collect the powder X-ray diffraction (XRD) patterns of the samples in a scanning range of $2\theta = 3^\circ - 30^\circ$. The voltage and current were 35 kV and 25 mA, respectively. The N $_2$ adsorption–desorption isotherms were measured on BELSORP-MAX adsorption instruments at 77.15 K after the samples were activated under vacuum at 623 K for 4 h in advance, which were employed to obtain the Brunauer–Emmett–Teller (BET) surface area and pore volume. The Si/Al ratios of the samples were determined using inductively coupled plasma optical emission spectroscopy (ICP-OES) analysis (Agilent 5110). The solid-state NMR spectra were obtained on a VARIAN VNMRS 400WB NMR spectrometer using the single-pulse method. The ^{27}Al MAS NMR spectra were recorded at 104.18 MHz, a spinning rate of 9 kHz, and a recycling delay of 4 s. The scanning electron micrographs (SEM) were performed on a Zeiss GeminiSEM450 prime at low landing energy (2 keV, in gentle-beam mode).

Temperature-programmed desorption of ammonia (NH $_3$ -TPD) on a Micrometrics Auto Chem II Chemisorption Analyzer was used to determine the zeolite acidity under He flow. Typically, 0.1 g sample in quartz tube was pretreated at 823 K for 1 h in flowing He gas, cooled to room temperature, and exposed to a 10% NH $_3$ /He mixture (30 mL·min $^{-1}$) for 1 h. Afterward, the sample was purged with He flow at 373 K for 30 min to remove physically adsorbed NH $_3$ on zeolite surface and NH $_3$ -TPD curves were collected in flowing He by raising the temperature from 323 to 773 K with a ramping rate of 10 K min $^{-1}$. The acid amounts were calculated based on the standard curve of the NH $_3$. In addition, the Lewis (LAS) and Brønsted acid site (BAS) contents were determined by the IR spectra after pyridine adsorption (Py-IR) on a Nicolet Nexus 670 instrument. All samples were pressed into self-supported wafers and degassed at 773 K for 1 h. Then, the wafers were exposed to pyridine vapor at ambient temperature for 10 min and then outgassed at 423 K for 30 min. Finally, the IR spectra were recorded at 423 K. The acid amount was calculated by $C = (IA \times S) / (W \times \epsilon)$, where C is the acid amount of LAS or BAS ($\mu\text{mol} \cdot \text{g}^{-1}$), IA is integral absorbance (cm^{-1}), S is the surface area of wafers (1.327 cm^2), W is the sample mass (g), and ϵ is absorptivity LAS or BAS ($\text{cm} \cdot \mu\text{mol}^{-1}$, $\epsilon_B = 1.67$, $\epsilon_L = 2.22$). The IR spectra of zeolite samples in hydroxyl-stretching region (OH-IR) were

collected at 423 K, after being activated under vacuum at 623 K for 1 h.

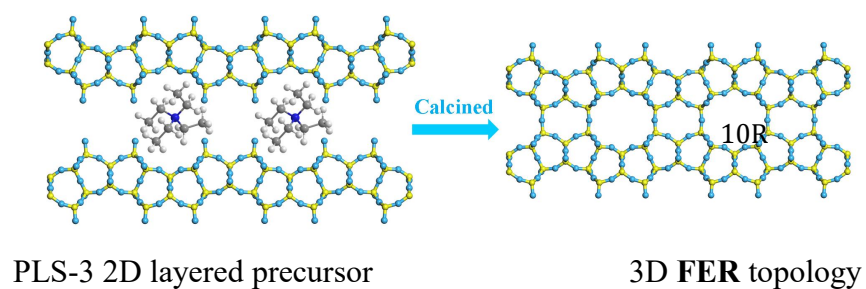
The in-situ IR spectra were collected on the Nicolet Nexus 670 with a reaction chamber to analyze the reaction mechanism. The sample were pressed into self-supported wafers and placed in the in-situ IR chamber and pretreated at 673 K for 2 h in He flow ($25 \text{ mL}\cdot\text{min}^{-1}$). Then, it was cooled to the reaction temperature to record the background spectrum. Subsequently, methanol (21.7 kPa at 303 K) was continuously introduced into the in-situ chamber under a CO/H₂ (volume ratio, 1 : 1) or N₂ flow ($25 \text{ mL}\cdot\text{min}^{-1}$). The IR spectra were collected at 623 K in the range of 4000 – 600 cm^{-1} .

Thermogravimetric–differential thermal analyses (TG) were performed on a METTLER TOLEDO TGA/DSC 3+ apparatus under air atmosphere ($50 \text{ mL}\cdot\text{min}^{-1}$), and 10 mg of each sample was subjected to the thermal analysis from 313 to 1073 K at a heating rate of $10 \text{ }^\circ\text{C}\cdot\text{min}^{-1}$. The organic hydrocarbons retained in the zeolite channels after the catalytic reaction of syngas conversion were analyzed using gas chromatography–mass spectrometry (GC-MS). The spent catalyst (25 mg) was dissolved in HF solution, and CH₂Cl₂ was used to extract the organic compounds. Then, CH₂Cl₂ solution was analyzed using an Agilent 6890 GC system equipped with a HP-5MS column and an Agilent 5977A Network Mass Selective Detector. The hydrocarbon content in the chromatograms was normalized with hexachloroethane as an internal standard for semi-quantitative analysis, and the species were identified by reference to the NIST08 mass spectral library using a literature method.^{2,3}



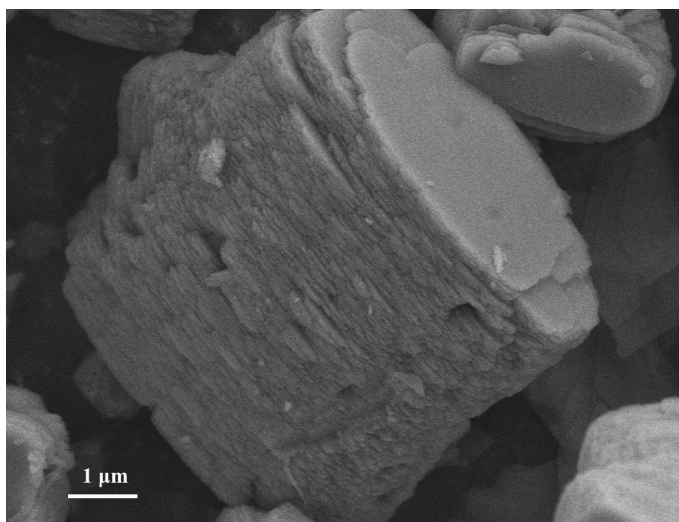
Supplementary Figure 1. The XRD patterns of silica source H-Kanemite and PLS-3 zeolite.

Note: Using layered silicate H-Kanemite as silica source, the PLS-3 lamellar aluminosilicate precursor was hydrothermally synthesized readily using TEAOH as OSDA. As-made PLS-3 showed the characteristic diffraction similar to layered PREFER,⁴ exhibiting the layer-related [200] diffraction at lower 2theta angle. After calcination and removal of occluded OSDA species, the interlayer condensation occurred, and the [200] diffraction peak shifted from 7.6° to 9.7°, resulting in 3D FER-type PLS-3 structure.

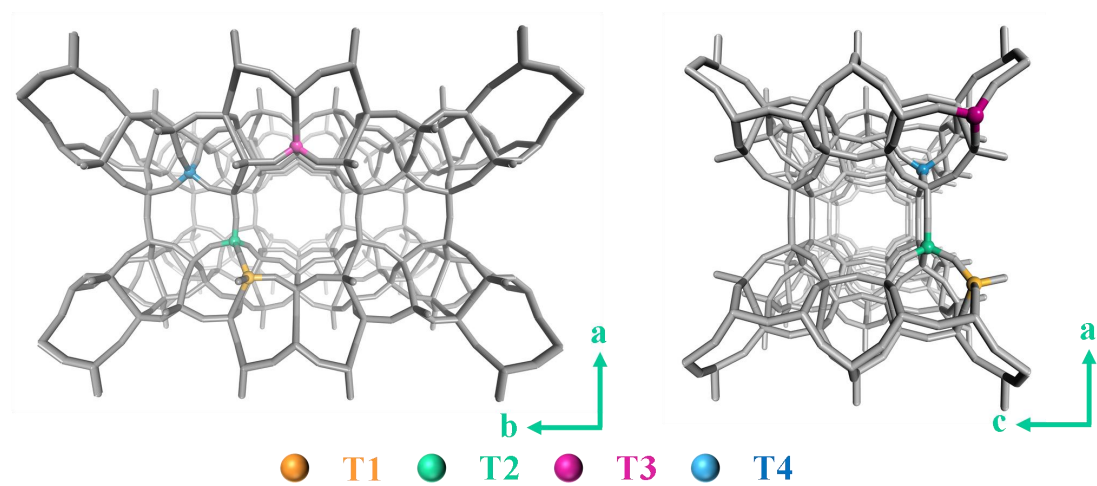


Supplementary Figure 2. Schematic illustration for topotactic transformation of PLS-3 lamellar precursor to 3D FER-type PLS-3 zeolite through calcination.

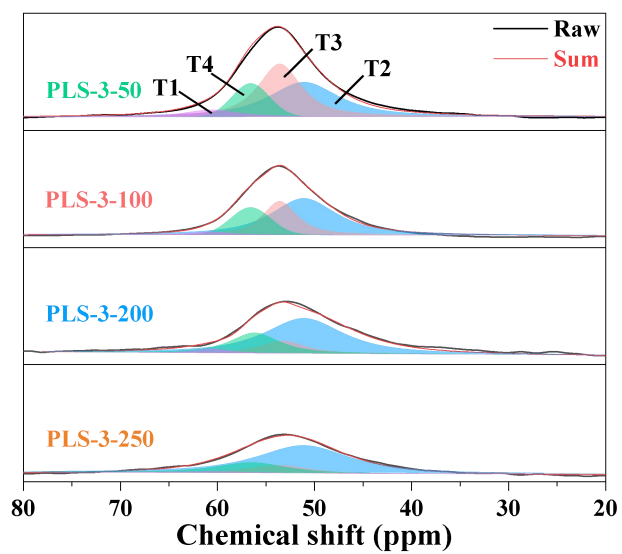
Note: The PLS-3 lamellar precursor with interlayer OSDA (TEA^+ species) experienced a topotactic transformation to 3D FER topology upon the calcination, due to the removal of occluded TEA^+ organic species accompanied by condensation of hydroxyl groups on the neighboring layers.



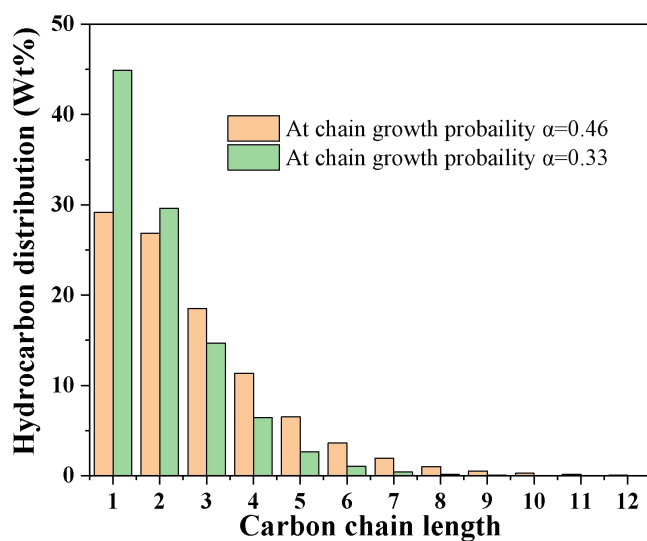
Supplementary Figure 3. Typical SEM image of conventional **FER** zeolite.



Supplementary Scheme 1. Geometric locations of nonequivalent T sites (T1-T4) in PLS-3 zeolite with the **FER** topology.

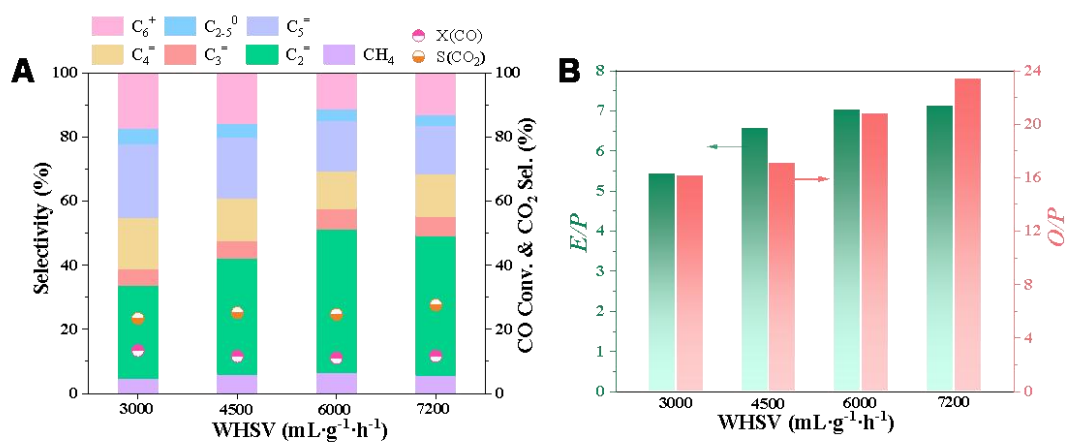


Supplementary Figure 4. ^{27}Al MAS NMR spectra of PLS-3 zeolites with different Si/Al ratios.

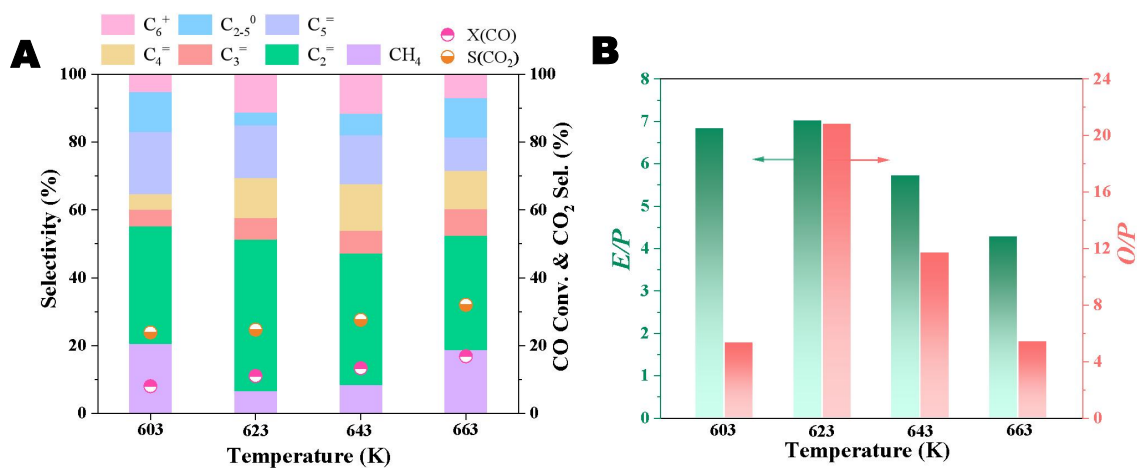


Supplementary Figure 5. The ASF model of Fischer-Tropsch synthesis. The hydrocarbon distribution with a carbon number of n depends on the chain growth probability (α) by the following equation: $W_n = n\alpha^{n-1}(1-\alpha)^2$, where W_n is the hydrocarbon distribution, α is chain growth probability, n is the carbon number.

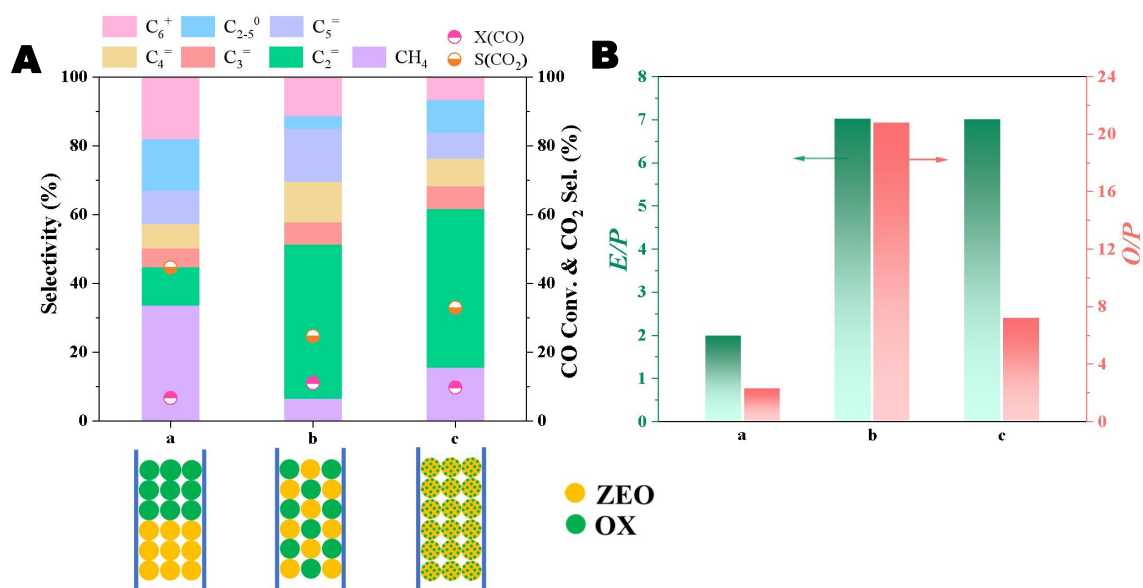
Note: The traditional Fischer-Tropsch synthesis (FTS) process follows the Anderson-Schulz-Flory (ASF) model,⁵ where the light hydrocarbon (C_{2-4}) selectivity does not exceed 58%. The C_{2-4} selectivity has exceeded 60% (Figure 5), and the single ethylene selectivity achieved 45% over the $Zn_2Al_3O_4/PLS-3$ catalysts, which breaks the ASF distribution.



Supplementary Figure 6. Effect of weight hourly space velocity (WHSV) on the catalytic performance of $\text{Zn}_2\text{Al}_3\text{O}_4/\text{PLS-3-250}$ (A). Dependence of E/P and O/P ratios on WHSV (B). Reaction conditions: catalyst mass, 0.25 g; metal oxide/zeolite mass ratio, 3 : 2; temperature, 623 K; pressure, 1 MPa; time on stream (TOS), 10 h.



Supplementary Figure 7. Effect of reaction temperature on the catalytic performance of Zn₂Al₃O₄/PLS-3-250 (A). Dependence of *E/P* and *O/P* ratios on reaction temperature (B). Reaction conditions: catalyst mass, 0.25 g; metal oxide/zeolite mass ratio of, 3 : 2; pressure, 1 MPa; the WHSV of syngas (H₂/CO volume ratio = 1 : 1), 6000 mL g⁻¹·h⁻¹; TOS, 10 h.



Supplementary Figure 8. Effect of mixing mode on the catalytic performance of $Zn_2Al_3O_4/PLS-3-250$ (A). Dependence of E/P and O/P ratios on the mixing mode of $Zn_2Al_3O_4$ and PLS-250 (B). Reaction conditions: catalyst mass, 0.25 g; metal oxide/zeolite mass ratio, 3 : 2; pressure, 1 MPa; temperature, 623 K; the WHSV of syngas (H_2/CO volume ratio = 1 : 1), $6000 \text{ mL g}^{-1}\cdot\text{h}^{-1}$; TOS, 10 h.

Supplementary Table 1. The catalytic performance of various metal oxide-zeolite bifunctional catalysts for the syngas conversion reaction from the reference

Catalyst	Ethylene Sel. (%)	O/P ratio	E/P ratio	Ref
ZnAlO _x /SAPO-34	17	5.5	0.37	6
ZnAlO _x /SAPO-17	32	4.7	1.18	
ZnAlO _x /SAPO-34	23	5.8	0.48	7
ZnAlO _x /SAPO-35	26	5.1	1.13	
ZnCrO _x /SAPO-34	23	5.6	0.50	8
ZnCrO _x /SAPO-34	23	5.7	0.51	9
ZnCrO _x / MOR-py	73	-	-	
MnO _x /MSAPO	-	5.5	-	10
ZnZrO/SAPO-34	-	2.76	-	11
ZnAlO _x /PLS-3	45	21.2	7.0	This work

Supplementary Table 2. Catalytic performance of Zn₂Al₃O₄/PLS-3-250 catalysts in syngas conversion reaction under different reaction conditions^[a]

Reaction condition	CO conv. (%)	CO ₂ sel. (%)	Product distribution (%)					DM E (%)	E/P	O/P	
			CH ₄	C ₂ ⁼	C ₂₋₅ ⁼	C ₂₋₅ ⁰	C ₆ ⁺				
WHSV (mL g ⁻¹ ·h ⁻¹)	3000	13.3	23.4	4.7	29.0	73.4	4.5	17.4	5.4	16.1	
	4500	11.5	25.2	5.9	36.1	74.1	4.3	15.7	6.6	17.1	
	6000	11.0	24.7	6.6	45.0	78.5	3.7	11.2	7.0	21.2	
	7200	11.7	27.6	5.7	43.6	77.9	3.3	13.1	7.1	23.6	
Temperature (K)	603	8.0	23.9	20.6	34.5	62.4	11.8	5.2	1.2	6.8	5.3
	623	11.0	24.7	6.6	45.0	78.5	3.7	11.2	7.0	21.2	
	643	13.3	27.6	8.4	38.8	73.7	6.3	11.6	5.7	11.7	
	663	16.8	32.0	18.8	33.6	62.7	11.6	6.9	4.3	5.4	

	Dual	6.7	44.6	33.7	11.0	33.3	15.0	18.0	3.4	2.0	2.2
Contact form	Granule	11.0	24.7	6.6	45.0	78.5	3.7	11.2		7.0	21.2
	Mortar	9.8	33.0	15.6	46.1	68.4	9.5	6.5		7.0	7.2

^[a] Reaction conditions: catalyst mass, 0.25 g; metal oxide/zeolite mass ratio, 3 : 2; pressure, 1 MPa; TOS, 10 h.

Reference

- (1) Tuo, J.; Fan, Y.; Wang, Y. et al. Promoting syngas to olefins with isolated internal silanols-enriched Al-IDM-1 aluminosilicate nanosheets. *Angew. Chem. Int. Ed.* **2023**, 62, e202313785.
- (2) Tuo, J.; Lv, J.; Fan, S. et al. One-pot synthesis of [Mn,H]ZSM-5 and the role of Mn in methanol-to-propylene reaction. *Fuel* 2022, 308, 121995.
- (3) Tuo, J.; Fan, S.; Yang, N. et al. Direct synthesis of [B,H]ZSM-5 by a solid-phase method: AlF siting and catalytic performance in the MTP reaction. *Catal. Sci. Technol.* 2020, 10, 7034-7045.
- (4) Yang, B.; Jiang, J.; Xu, H.; et al. Selective skeletal isomerization of 1-butene over FER-type zeolites derived from PLS-3 lamellar precursors. *Appl. Catal. A: Gen.* **2013**, 455, 107-113.
- (5) Zhou, W.; Cheng, K.; Kang, J. et al. New horizon in C1 chemistry: breaking the selectivity limitation in transformation of syngas and hydrogenation of CO₂ into hydrocarbon chemicals and fuels. *Chem. Soc. Rev.* **2019**, 48, 3193-3228.
- (6) Ni, Y.; Liu, Y.; Chen, Z. et al. Realizing and recognizing syngas-to-olefins reaction via a dual-bed catalyst. *ACS Catal.* **2019**, 9, 1026-1032.
- (7) Wang, M.; Kang, J.; Xiong, X. et al. Effect of zeolite topology on the hydrocarbon distribution over bifunctional ZnAlO/SAPO catalysts in syngas conversion. *Catal. Today* **2021**, 371, 85-92.
- (8) Jiao, F.; Li, J.; Pan, X. et al. Selective conversion of syngas to light olefins. *Science* **2016**, 351, 1065-1068.
- (9) Jiao, F.; Pan, X.; Gong, K. et al. Shape-selective zeolites promote ethylene formation from syngas via a ketene intermediate. *Angew. Chem. Int. Ed.* **2018**, 57, 4692-4696.
- (10) Zhu, Y.; Pan, X.; Jiao, F.; Li, J.; Yang, J.; Ding, M.; Han, Y.; Liu, Z.; Bao, X. Role of Manganese Oxide in Syngas Conversion to Light Olefins. *ACS Catal.* **2017**, 7, 2800-2804.
- (11) Cheng, K.; Gu, B.; Liu, X.; Kang, J.; Zhang, Q.; Wang, Y. Direct and Highly Selective Conversion of Synthesis Gas into Lower Olefins: Design of a Bifunctional Catalyst Combining Methanol Synthesis and Carbon–Carbon Coupling. *Angew. Chem. Int. Ed.* **2016**, 128, 4803-4806.